ECRH PREIONIZATION IN TOKAPOLE II

D. Holly
D. Witherspoon
J.C. Sprott

PLP 774

December 1978

Plasma Studies

University of Wisconsin

ECRH preionization of a tokamak has been suggested as a way to reduce the startup voltage and the initial impurity influx, as the cyclotron resonance zone can be positioned where desired. We have initiated ohmic discharges in Tokapole II using 10 kW of 8.8 GHz ECRH and find that the ECRH preionization causes the impurity radiation to drop by as much as 50%.

Waveforms for a typical Tokapole II shot are shown in Fig. 1. Note that the preionization takes place in a purely toroidal field which is roughly constant in time, so that the ECRH resonance zones are vertical cylinders centered on the major axis. Langmuir probe traces, taken with no poloidal (i.e., ohmic heating) field (Fig. 2), show that the plasma peaks at the ECRH resonance zone as expected. There is also significant plasma density (25% to 50% peak density) from the resonance zone to the outer wall. Photographs of the discharge (Figs. 3, 4, 5) also clearly show the plasma peaked at the resonance zones.

However, when a small amount of toroidal ohmic heating is added (Fig. 6), Langmuir probe traces show very little difference between the ECRH-preionized case and the non-preionized case once the ohmic discharge has started. Photographs of the plasma in these cases also show little or no difference.

While we were not able to monitor a standard tokapole discharge with a Langmuir probe (the probes then in use melted when we attempted it), other diagnostics indicate that the ECRH preionization does have an effect on the tokapole discharge. Figure 7 shows the decrease in vacuum ultraviolet (impurity) radiation and the increase in copper radiation due to the preionization. Note that as the ECRH power was varied from 1 kW to about 10 kW, there was very little change in the effect produced by the preionization on the tokapole discharge (Fig. 8).

The vacuum UV radiation was monitored by a 1/2-m Seya monochromator with a channeltron array in place of the exit slit; the current to the channeltron

array then was proportional to the VUV radiation intensity integrated over wavelengths from about 500 Å to 1300 Å. The monochromator was aimed at the center of the discharge, along the major radius. As shown in Figs. 7 and 8, ECRH preionization reduced the vacuum UV signal, indicating that initial impurity influx had been reduced by the preionization.

We moved the resonance zone across the machine by varying the peak toroidal field strength. Figure 9 shows the effect of resonance zone location on the impurity radiation. Since the tokapole discharge parameters vary with B_T in addition to the variation due to the ECRH zone, we plotted (Fig. 10) the percent change in the vacuum UV signal with/without ECRH preionization as the resonance zone was moved across the machine by varying B_T. Note that the ECRH preionization produces the biggest reduction in impurity radiation (50%) when the ECRH resonance zone intersects the hoops. One might have expected instead the biggest impurity reduction when the resonance zone was placed at the minor axis.

Cu I radiation is monitored by a photomultiplier tube which views the plasma through a narrow-band optical filter and through a long movable collimating tube. This was aimed near the outer hoop. A large increase in Cu I radiation is observed when the resonance zone is positioned near the outer hoop (Fig. 11). Note that this increase persists throughout the plasma lifetime (second photo of Fig. 7). Also note that a smaller peak in Fig. 10 occurs when the resonance zone intersects the inner hoop.

The gross plasma parameters, such as plasma current and electron temperature, are less affected by the preionization. The preionization produced no observable effect on runaway electron production, as monitored by a hard x-ray detector. Figure 12 shows the effect of ECRH preionization on $\int I_p dt$, a quantity which is related to T_e and which is used as a figure of merit of tokapole discharges. Note that the increase with ECRH preionization is never more than about 15% and shows no structure as the resonance zone is swept across the machine. The

increase in $\int I_p dt$ with preionization may be due mostly to earlier starting of the plasma discharge with preionization and not to limiting impurity influx. This is consistent with the belief, based on quantitative radiation measurements, that impurity radiation is not a major limitation in present Tokapole II discharges.

Although ECRH preionization has only a small effect on tokapole discharges, this is not to say that it would not produce significant improvements in a tokamak without a poloidal divertor. The poloidal divertor coils (hoops in our case) may produce a central current channel with a stable equilibrium, thereby accomplishing the same result as ECRH preionization.

A TYPICAL TOKAPOLE II SHOT

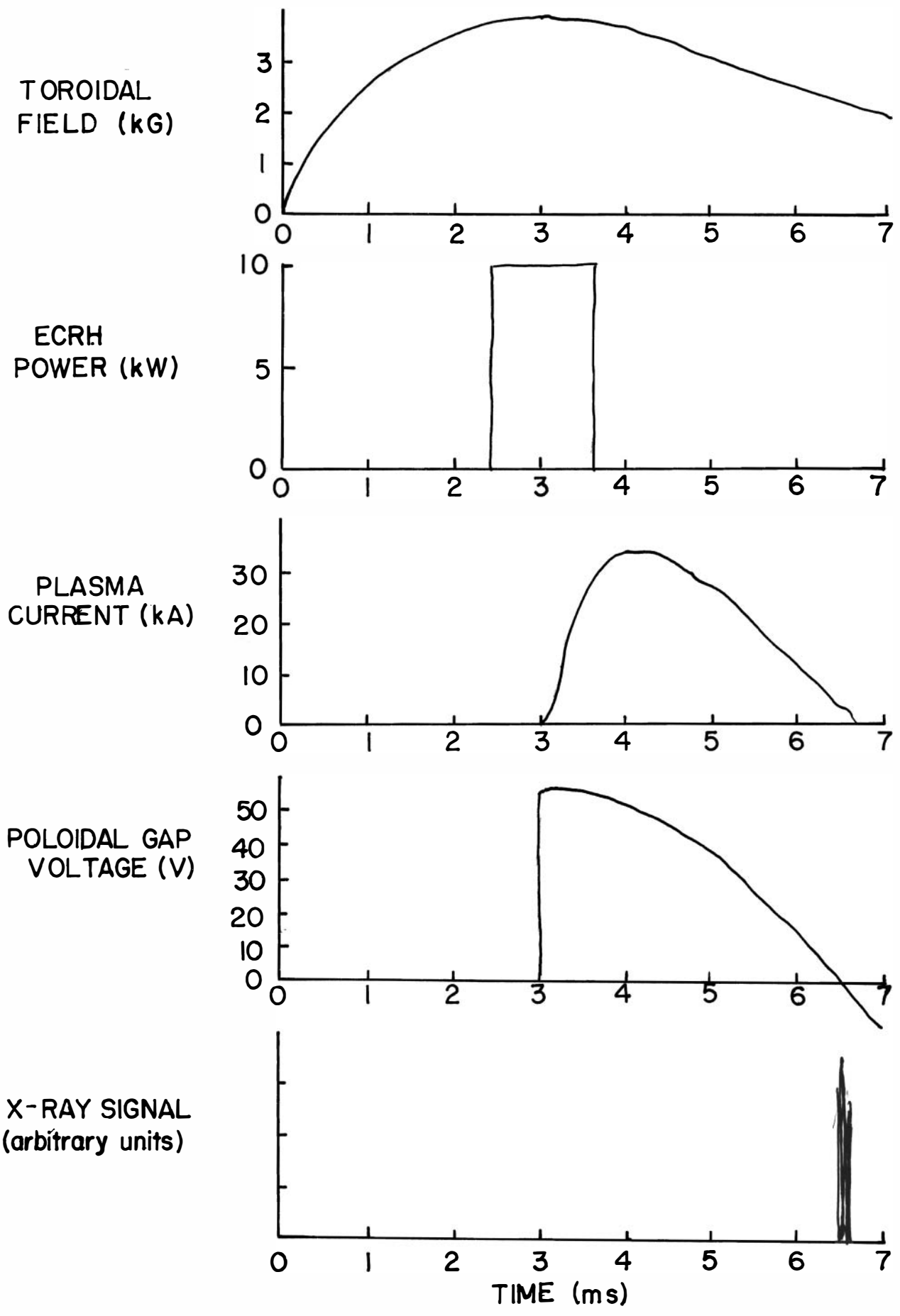

Fig. 1

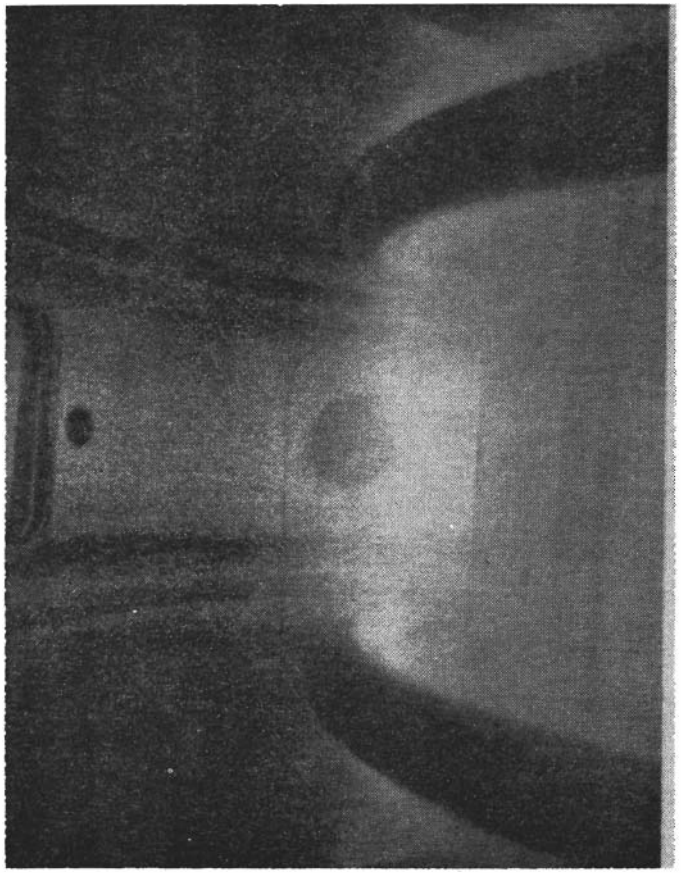

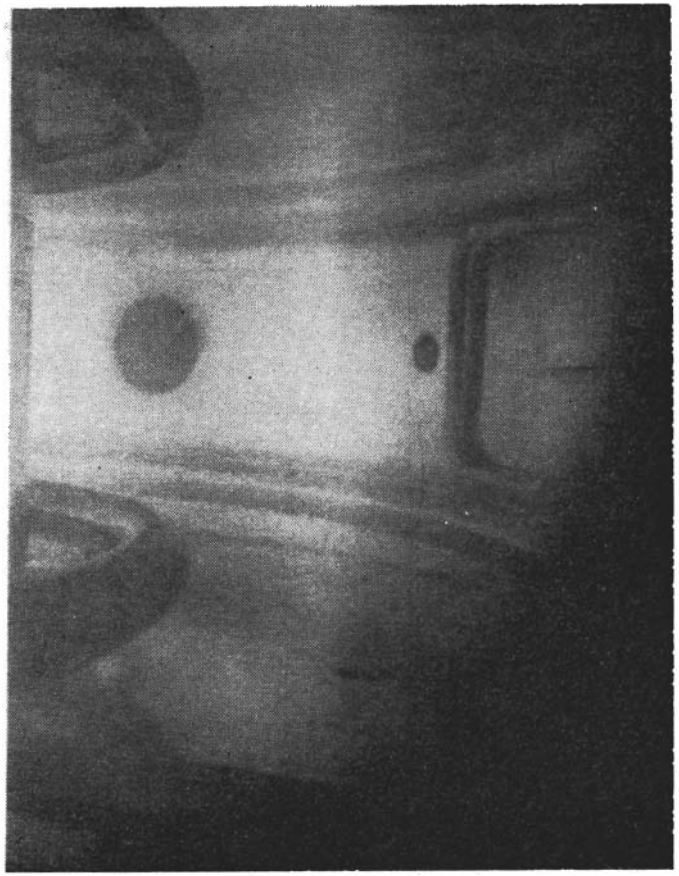

THESE ARE
THE BEST REPRODUCTIONS!

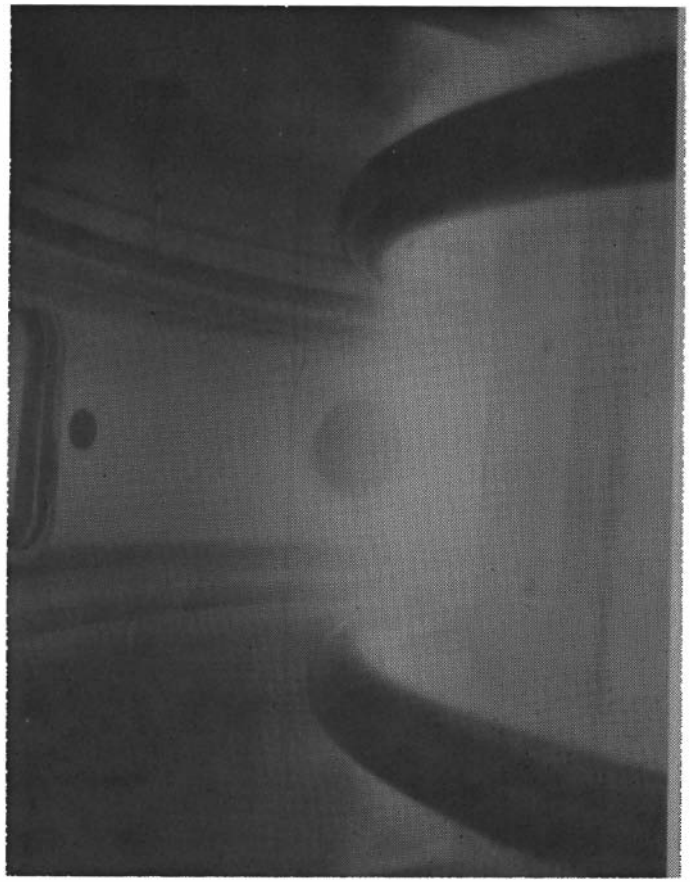

Fig. 3. B_T on axis = 2.32 kG.

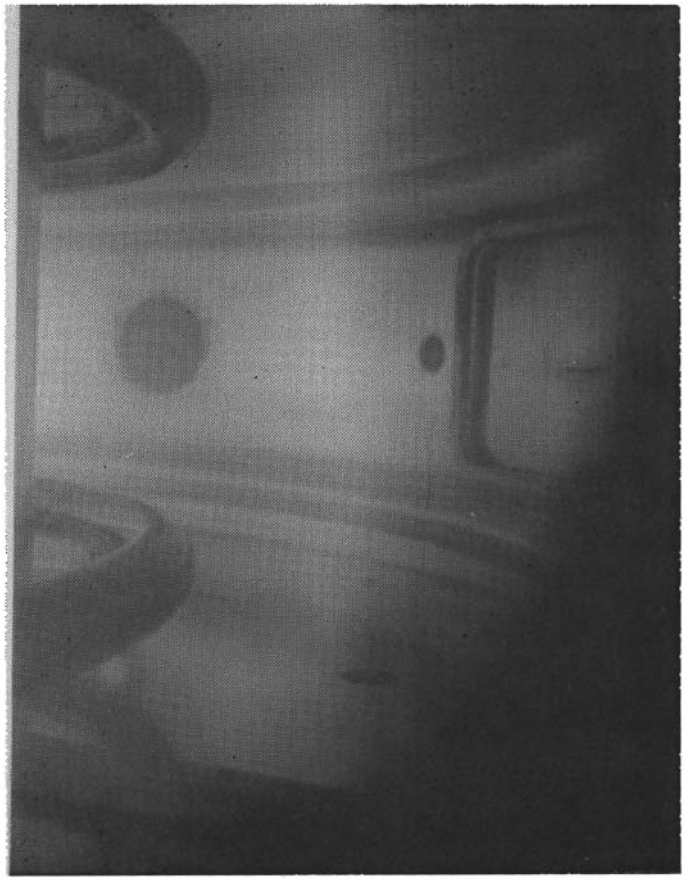

Fig. 4. B_T on axis = 3.15 kG.

Fig. 5. B_T on axis = 3.87 kG.

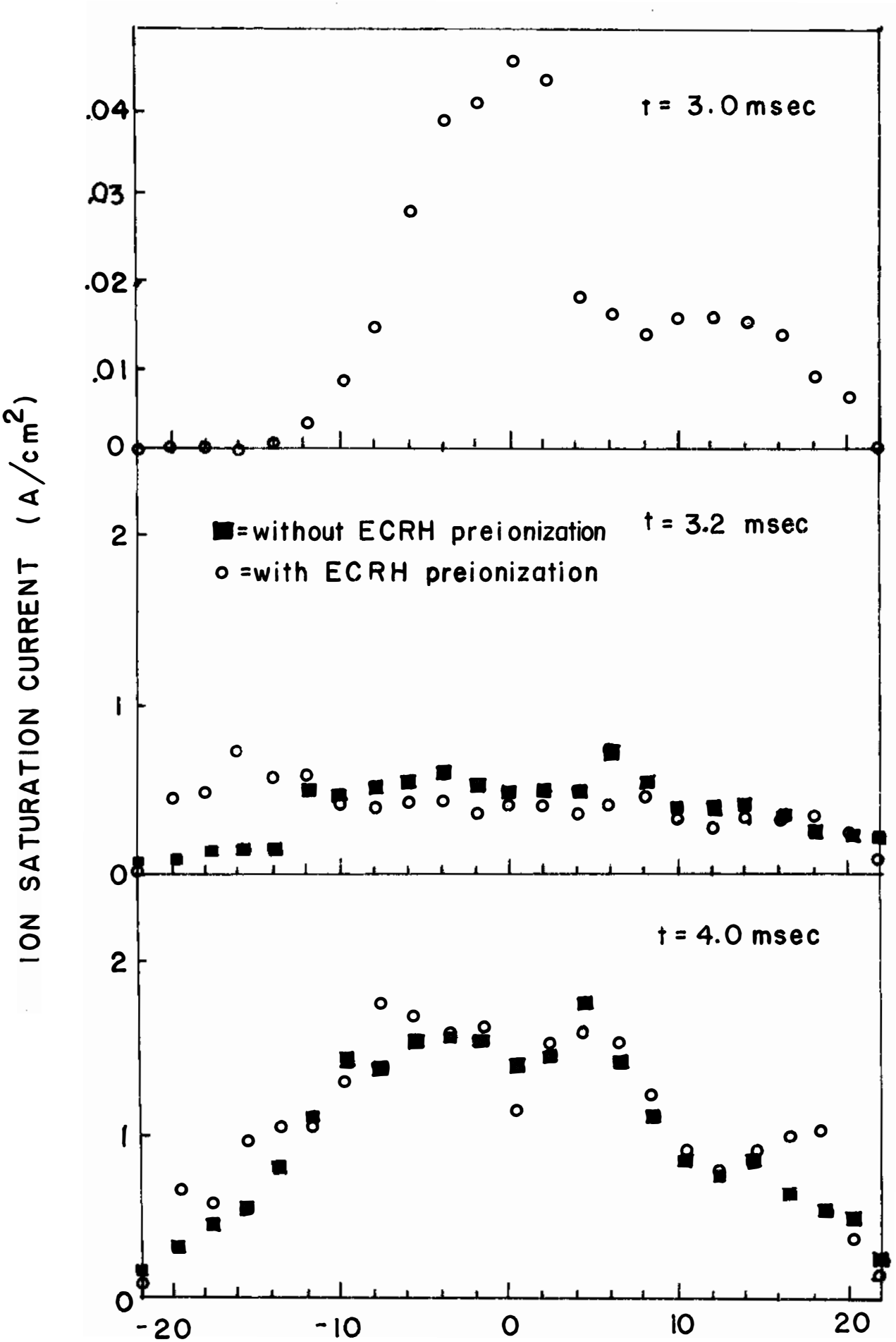
t = 3.0 msec
t = 3.2 msec
■ = without ECRH preionization
o = with ECRH preionization
t = 4.0 msec
ION SATURATION CURRENT (A/cm²)
DISTANCE FROM MINOR AXIS (cm)
.04
.03
.02
.01
0
2
1
0
2
1
0
-20
-10
0
10
20

Fig. 6

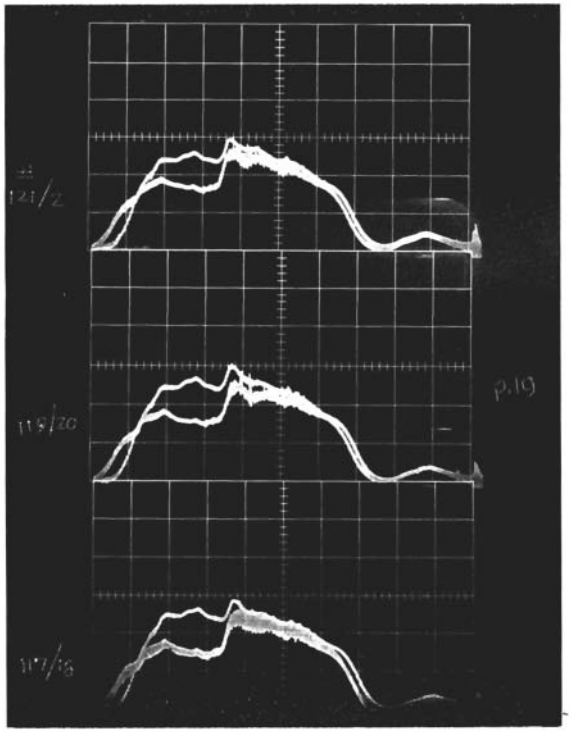

VACUUM UV RADIATION
HORIZONTAL .5 MSEC/DIV

THE UPPER CURVE IN EACH OF THE 3 TRACES IS WITHOUT ECRH PREIONIZATION; THE LOWER CURVE IS WITH ECRH PREIONIZATION.

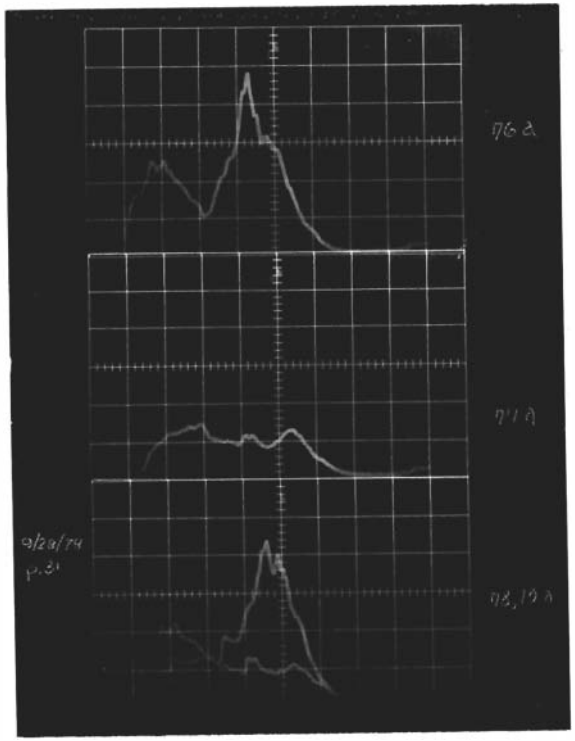

Cu I RADIATION
HORIZONTAL .5 MSEC/DIV

THE TOP TRACE IS WITH ECRH PREIONIZATION; THE CENTER TRACE IS WITHOUT ECRH PREIONIZATION. THE BOTTOM TRACE IS A SUPERIMPOSITION OF THE TWO.

Fig. 7

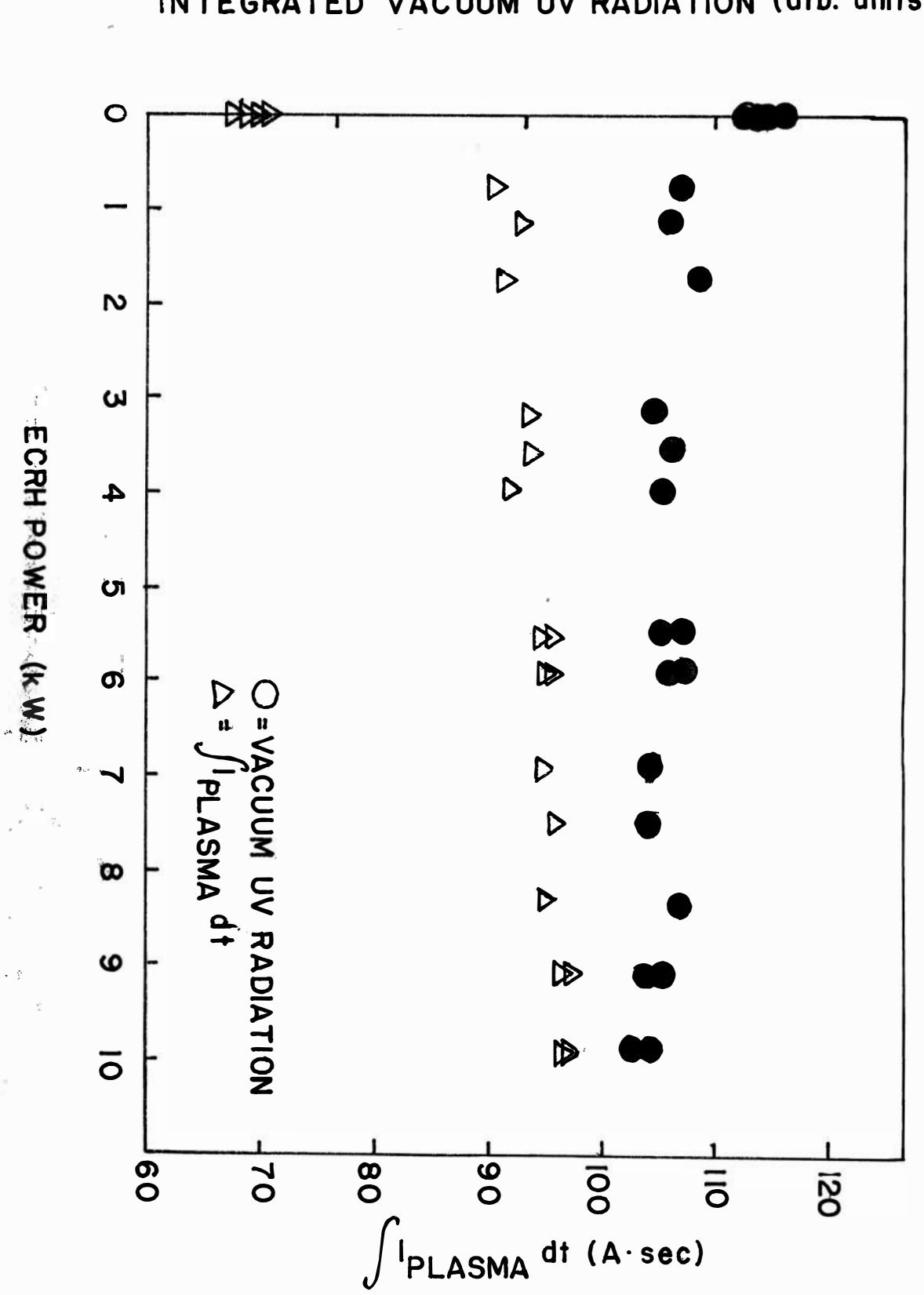
INTEGRATED VACUUM UV RADIATION (arb. units)
ECRH POWER (k W)
0
1
2
3
4
5
6
7
8
9
10
O = VACUUM UV RADIATION
Δ = ∫ I PLASMA dt
60
70
80
90
100
110
120
∫ I PLASMA dt (A · sec)

Fig. 8

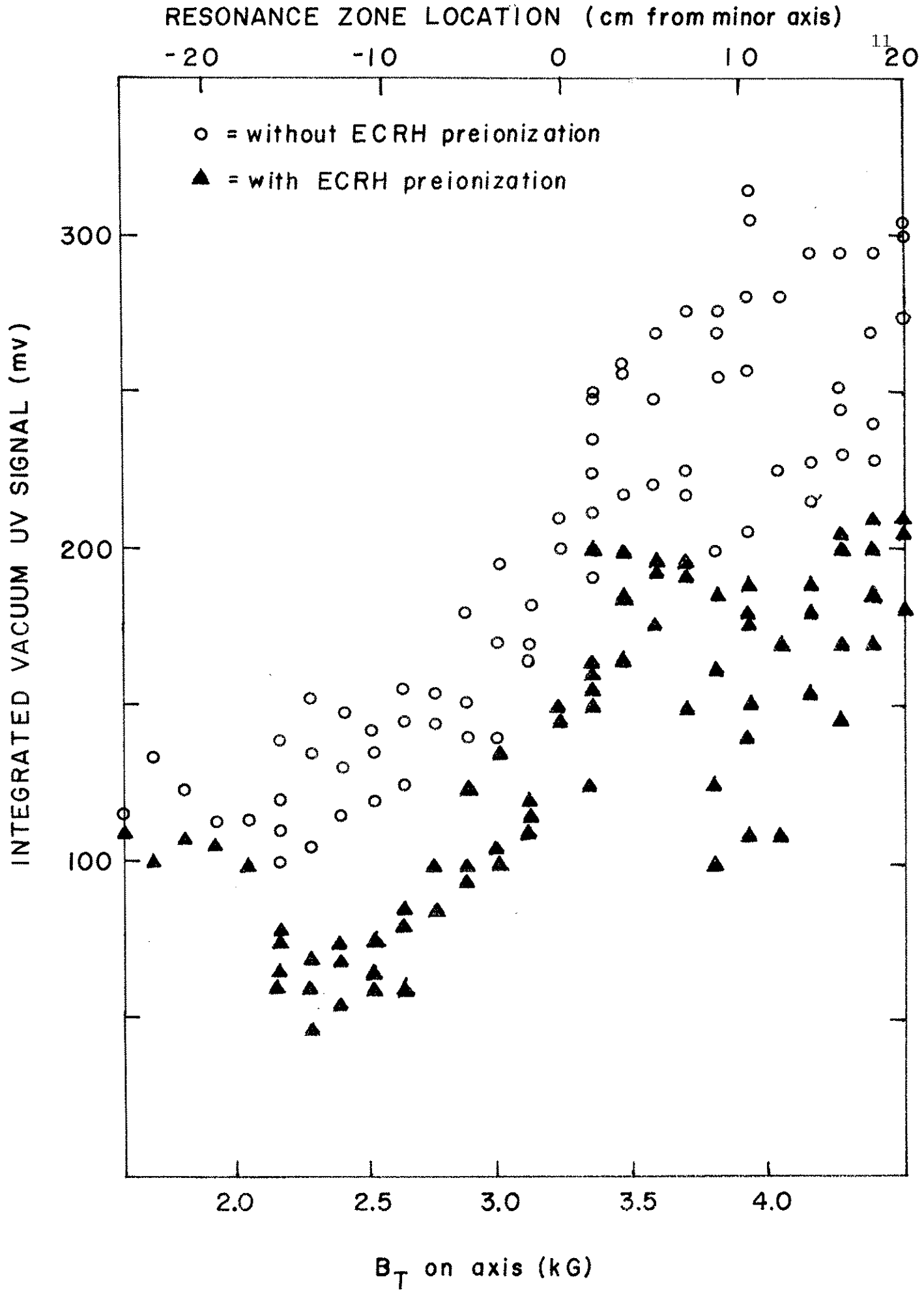
RESONANCE ZONE LOCATION (cm from minor axis)
-20
-10
0
10
20
o = without ECRH preionization
▲ = with ECRH preionization
300
200
100
INTEGRATED VACUUM UV SIGNAL (mv)
2.0
2.5
3.0
3.5
4.0
B_T on axis (kG)

Fig. 9

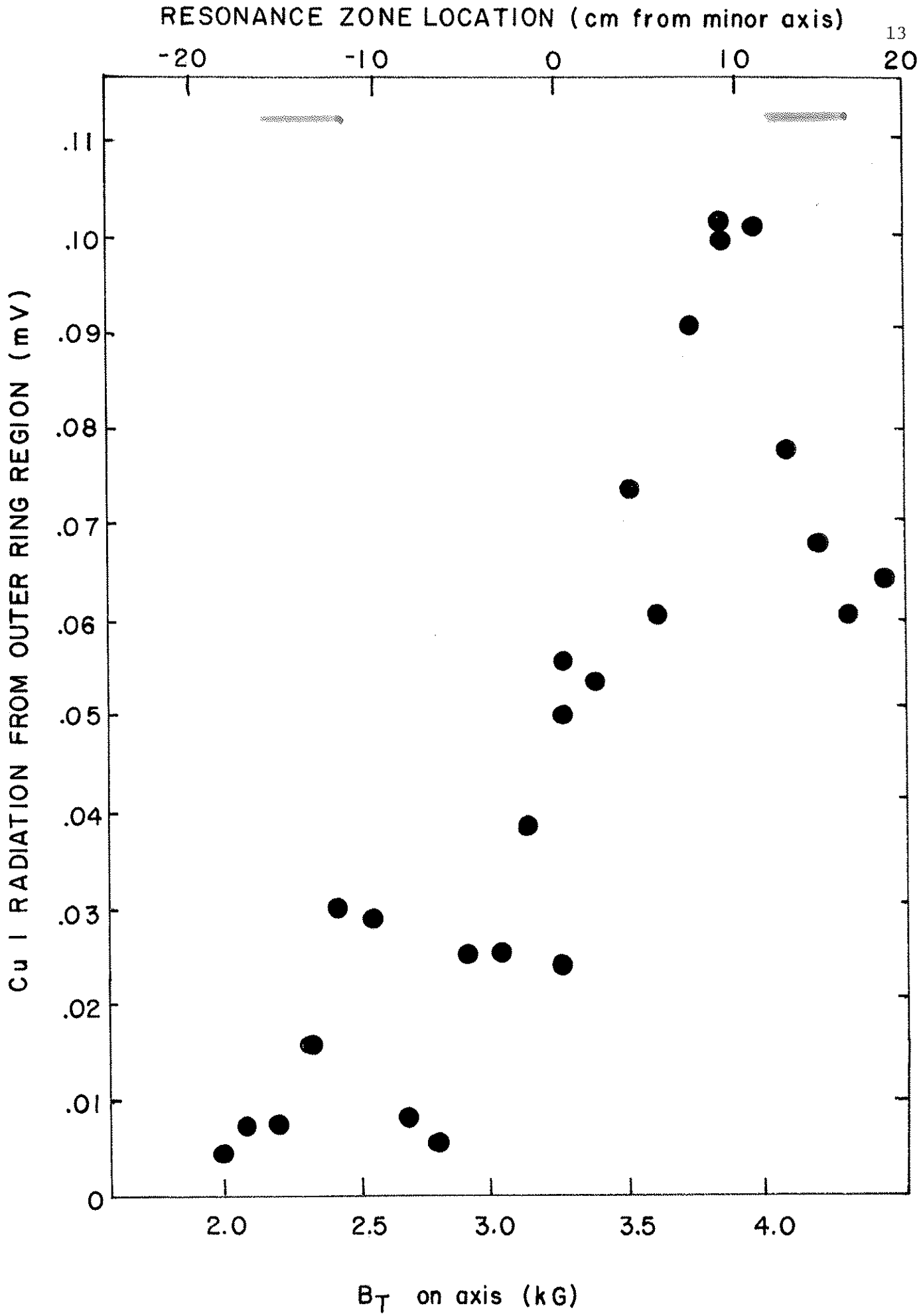
RESONANCE ZONE LOCATION (cm from minor axis)
-20
-10
0
10
20
.11
.10
.09
.08
.07
.06
.05
.04
.03
.02
.01
0
Cu I RADIATION FROM OUTER RING REGION (mV)
2.0
2.5
3.0
3.5
4.0
B_T on axis (kG)

Fig. 11

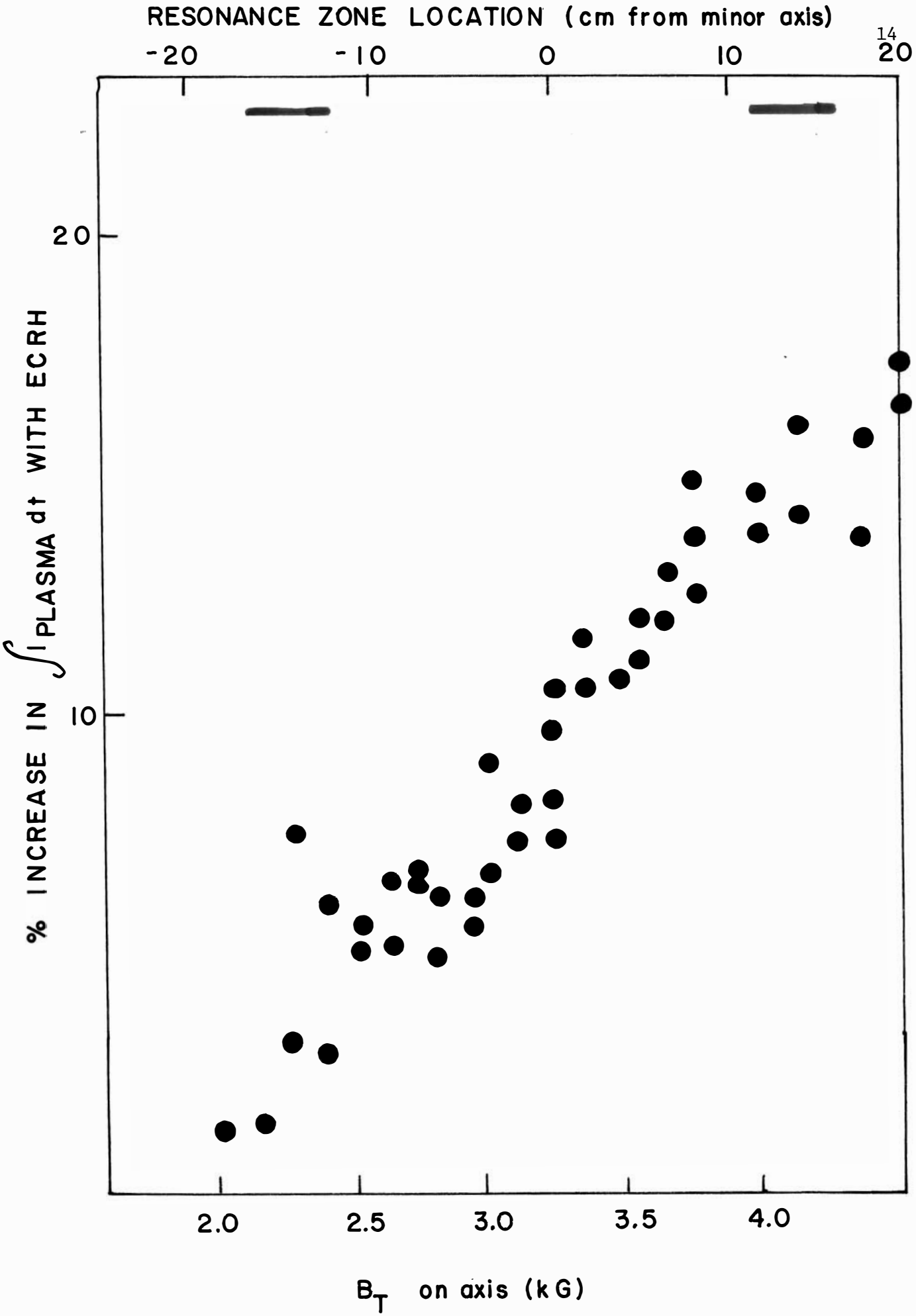
RESONANCE ZONE LOCATION (cm from minor axis)
-20
-10
0
10
20
20
10
% INCREASE IN $\int I_{PLASMA}\,dt$ WITH ECRH
2.0
2.5
3.0
3.5
4.0
B_T on axis (kG)

Fig. 12